AUTOMATIC FACADE IMAGE RECTIFICATION AND EXTRACTION USING LINE SEGMENT FEATURES

Chun Liu
INRIA Rocquencourt, Domaine de Voluceau, 78153 Le Chesnay, France

Keywords: Perspective rectification, Line segment detection, Image segmantation, Markov random field, Symmetry detection.

Abstract: Recently image based facade modeling has attracted significant attention for 3D urban reconstruction because of low cost on data acquisition and large amount of available image processing tools. In image based facade modeling, it normally requests a rectified and segmented image input covering only the facade region. Yet this requirement involves heavy manual work on the perspective rectification and facade region extraction. In this paper, we propose an automatic rectification and segmentation process using line segment features. The raw input image is firstly rectified with the help of two vanishing points estimated from line segment in the image. Then based on the line segment spatial distribution and the luminance feature, the facade region is extracted from the sky, the road and the near-by buildings. The experiments show this method successfully work on Paris urban buildings.

1 INTRODUCTION

Urban modeling is becoming an intense research topic because of practical interests and usages in several areas such as tourism, environment, military, economy, etc. Among all methodologies for obtaining 3D city representations, image based approach is preferred most because this approach offers low cost and has a lot of flexibility. This image based approach involves detecting and recognizing the overall structure of a building and the individual elements from 2D ground images, which will be used later for 3D reconstruction of the cities.

The first step in image based modeling procedure (see figure 1) is to rectify the raw image against the perspective distortion and to extract region of interest. Upon the completion of this process, a rectified and a much cleaner image input with less distortion and interference from unrelated image content is produced. This way, the determination of building structure and the recognition of various building elements become much easier and more straightforward.

However less research work has been done on the automation of this process. This is due to the fact that the urban scenes have added many layers of complexity into the process automation. And usually this task is left to the manual processing in most interactive modeling softwares. Consequently, in the large scale urban modeling with numerous facade images, the manual rectification and extraction process can be heavy and painful for the human modelers.

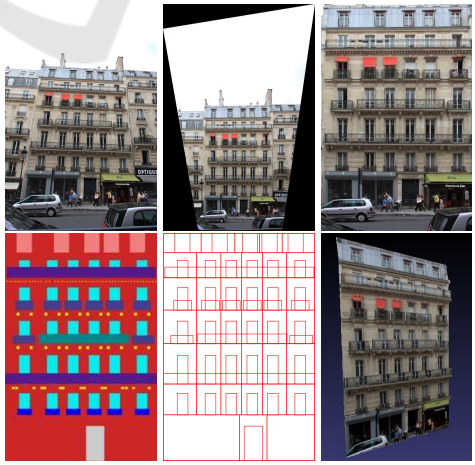

Figure 1: Modeling Procedure. left to right, up to down, original image, rectified image, segmented facade image, image semantic segmentation, geometry detection, final model.

This paper describes an unsupervised automatic process for rectification and extraction of complex facade images in Paris urban area. In this process, we first extract line segments from the image and then estimate the horizontal and vertical vanishing points.

Liu C..
AUTOMATIC FACADE IMAGE RECTIFICATION AND EXTRACTION USING LINE SEGMENT FEATURES.
DOI: 10.5220/0003316401040111
In *Proceedings of the International Conference on Computer Vision Theory and Applications* (VISAPP-2011), pages 104-111
ISBN: 978-989-8425-47-8

The line segment is defined as the edge with a precise length. Using the two vanishing points, the homography matrix which defines the image projection is estimated and the image is rectified. Next in the rectified image, the unwanted regions such as the sky, the road and the neighbourhood area are recognized by using the line segment spatial distribution and the luminance features. As a result, the region of interest where the building facade locates is extracted for further analysis tasks.

The assumption and the requirement for this method is that the facade images need to be taken in a cloudy morning, or evening, of later Spring or early Autumn, when the building facades are relatively illuminated homogeneously and less occluded by vegetation. In addition, the image needs to be taken with large angle objective so the facade will be contained in one single image. These restrictive conditions ensure that the facade image will preserve maximum details and different parts of the facade can be relatively easy to differentiate in terms of geometry, color and texture.

1.1 Related Work

The perspective rectification and image segmentation for natural and urban scene interpretation have been studied intensively in computer vision.

The general procedure for the interpretation involves three steps, feature extraction, feature processing based on mathematical modeling of the problem and the final inference. The selection of features are crucial and problem-specific. The widely used features include shape, color and textures. Those visual appearances are extracted straightforwardly and compared directly using various error metrics. However, in complicated urban scenes, where human made objects could be highly textured and occluded, those visual appearance features are not suitable for direct comparison. For instance, a blazing window glass can reflect any visual content from the sky or neighbourhood which is interfering and not related to the true characteristics so that two identical windows may appear different visually.

The edges, which are the discontinuities over the borders of objects on images, can provide strong clues for object shape and location information. This is especially apparent in man-made objects where many rectangular surfaces exist such that horizontal and vertical edges are often seen. For complex shape detection, one can take advantage of processing edges elaborately. Similarly, proper clustering of the edges can be utilized to analyze the overall typology of the man made objects such as architectures where repetition and symmetry of primitive geometries are the typical composition characteristics. In addition, the distribution of edges could reveal other useful information such as the orientation of the scene.

Traditionally, the detection of line segment, is based on edge detection and the Hough transform (Matas et al., 1998). And the line segment hypothesis is usually validated by hard decisions on the gap and length thresholds. As a result, this detection often produces false line segments, which can be harmful to further edge feature processing. Rafael et al (Grompone von Gioi et al., 2010) proposed a fast line segment detection algorithm which provides almost no false line and the computation time is linear. This algorithm takes gradient as input and searches for line region by considering less false detection. The output from this algorithm is close to human perception such that in case of a noisy like texture, there will be no line segment detected. With this line segment detector, the line segment is robust and less biased for computer vision problems.

In processing architectural photos, the successful perspective rectification depends on accurate estimation of vanishing points, which are intersecting points from line segments on images. In highly rectangular textures (Liebowitz and Zisserman, 1998), lines can be easily extracted and rectification is completed by combining affine rectification with vanishing points and metric rectification with other priors like known angles between lines. However, generally, such prior information can not be obtained automatically and needs human interaction. In general case (Kalantaria et al., 2008), the image is rectified by using two vanishing points and solving the homography matrix directly. The certainty of less interference from false line detection is provided by using RANSAC algorithm. However, the rectification is less efficient due to abundant false line segments.

The segmentation of outdoor scene could also benefit from line segment detection. Derek Hoeim (Hoiem et al., 2005) proposed a decision tree based machine learning algorithm for outdoor scene segmentation. In his method, the direction of edges is considered as key feature and was shown to provide useful information in differentiating objects. Despite the method's general application, the amount of manual labeling work can be terrifying. Similarly in the unsupervised approaches, the interpretation of the sky can rely on edge analysis (Laungrungthip et al., 2008). In this case, the sky can be thought of as clean regions against the ground, different to previous assumption that the sky is more blue than the ground (Laungrungthip, 2008) (Schmitt and Priese, 2009) (Zafarifar and de With, 2006).

The removal of the ground from the outdoor scene is also of interest in automobile navigation. Most literature in road detection have described using photos taken from the air (Quartulli and Datcu, 2004) or from road vehicles in which case the road is in the center of the image. There are less works on road detection on static building photos because the ground-level urban scene is too complex to analyze. Therefore, the detection of road will need more computation-intensive detection of pedestrians and cars.

The subsequent sections are organized as follows. Section 2 discusses the line segment features and its advantage against the conventional edge features. Section 3 describes the perspective rectification procedure. Section 4 presents how the facade region is extracted from backgrounds such as the sky, the ground and the neighbourhood. Section 5 provides the results and the conclusion.

2 LINE SEGMENT FEATURES

Line Segment features provide more precise information of object geometries on images. In complex urban scene, where luminance and occlusion can not be controlled, line segments can reveal the image discontinuity over the object borders with strong confidence compared to other regional features such as color and texture. Moreover, the use of specific line segment detection (Grompone von Gioi et al., 2010), has allowed the robust estimation of object geometry. Figure 2 shows the comparison of line segment detection with other edge detection methods.

Line segments can also be used to discover the high level structure information of an image. The spatial distributions of line segments can indicate more clues such as the existence or the discontinuity of repetition and symmetry. Figure 2 clearly shows that, the separation for floors, tiles and facades can be determined from horizontal and vertical line segment detections. Furthermore, the orientation of the scene can also be determined since all the horizontal lines are converging to the left. This line segments convergence will in turn indicate the location of the vanishing point, which is useful for perspective rectification.

3 PERSPECTIVE RECTIFICATION

In computer vision, the mapping of object (building facades) 3D coordinates onto the imager of the camera is a planar homography. Denote the points from

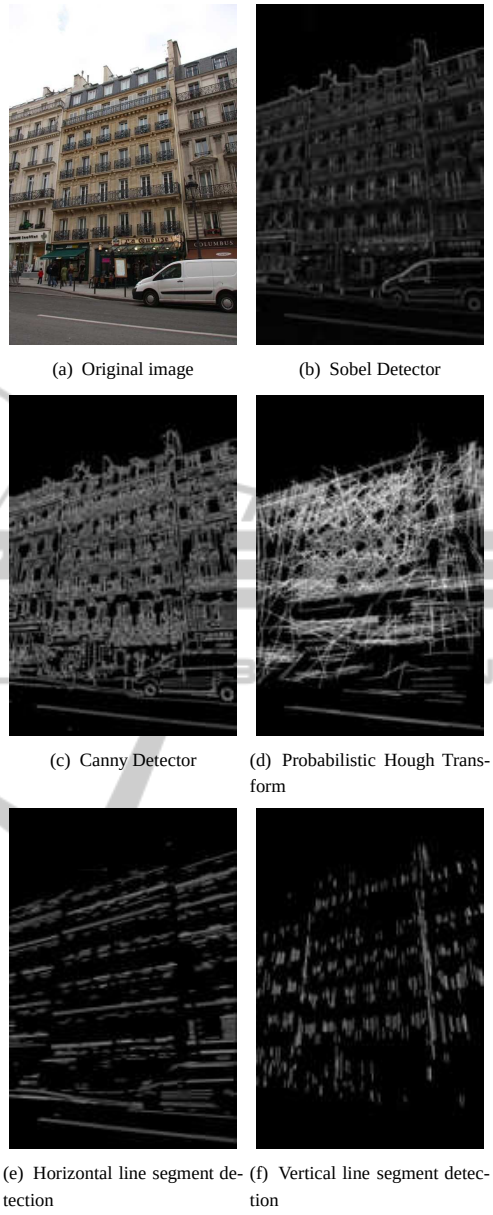

(a) Original image (b) Sobel Detector

(c) Canny Detector (d) Probabilistic Hough Transform

(e) Horizontal line segment detection (f) Vertical line segment detection

Figure 2: Edge Detection vs Line Segment Detection.

building facades in the real world as $\vec{P^w}$, and pixels on images as $\vec{P^i}$, we have the homography as below:

$$\vec{P^i} = \begin{pmatrix} h_{11} & h_{12} & h_{13} \\ h_{21} & h_{22} & h_{23} \\ h_{31} & h_{32} & h_{33} \end{pmatrix} \vec{P^w} \qquad (1)$$

where h_{33} is set to 1.0 and $\vec{P^w}$, $\vec{P^i}$ are in $\mathbb{R}^3$, $\vec{P^w} = [a^w x^w, a^w y^w, a^w]^T$, a is scaling factor, $\vec{P^i} = [x^i, y^i, 1.0]^T$. The homography H has eight degrees of freedom. Therefore, eight equations are needed to determine all the coefficients. Given four point cor-

respondences, image points (x_k^i, y_k^i). and points in the real world (x_k^w, y_k^w), $k = 0, \ldots, 3$, H will be determined.

Provided the vanishing points which we assume to consist of two points, one is for the horizontal vanishing point and the other is for the vertical vanishing point, it is possible to construct four point correspondences between the real world (the scaling factor a is set to 1.0) and image.

3.1 Rectification Process

Considering vanishing points configuration as figure 4. $VP0$ is the horizontal vanishing point and $VP1$ is the vertical vanishing point. Then we project lines from the vanishing points to the image. Subsequently, they will intersect at four points around the image, A, B, C and D. In real world, horizontal lines AC and BD should be parallel, and so do vertical lines AB and CD.

As a result, if we can wrap the four lines AC, BD, AB and CD back to the four lines defining the image frame rectangles, the image will be rectified such that all lines pointing to the same vanishing points are converted back to be parallel. By applying this 2D wrapping (the Z coordinate in the real world is set to 1.0), the image is rectified. Considering this wrapping, the four points correspondences between A, B, C, D and four image corners, $upper\_left$, $upper\_right$, $lower\_left$, $lower\_right$ can be used to determine the homography matrix.

3.2 Vanishing Points Estimation

The procedure starts from line segment detections. On the facade image, the horizontal and the vertical line segments are picked up with proper angle quota between the line and the image width axis. The horizontal lines should have angles smaller than 45° while the vertical lines should have angles larger than 45°.

After line segment extraction, the estimation of vanishing points is done in horizontal and vertical direction separately but follows the same procedure. The initial vanishing point estimation is taken by calculating the mean point of intersecting points from every non-parallel line segments. Next, the Levenberg Marquardt optimization is performed to estimate the optimal vanishing point location by checking how the vanishing point fits every line segment. However, due to image distortion, image noise, and line segment perturbation not pointing to the vanishing points from non rectangular objects on the facades, the optimization result from line segments is biased. Therefore, we need to use RANSAC (see Algorithm 1) to

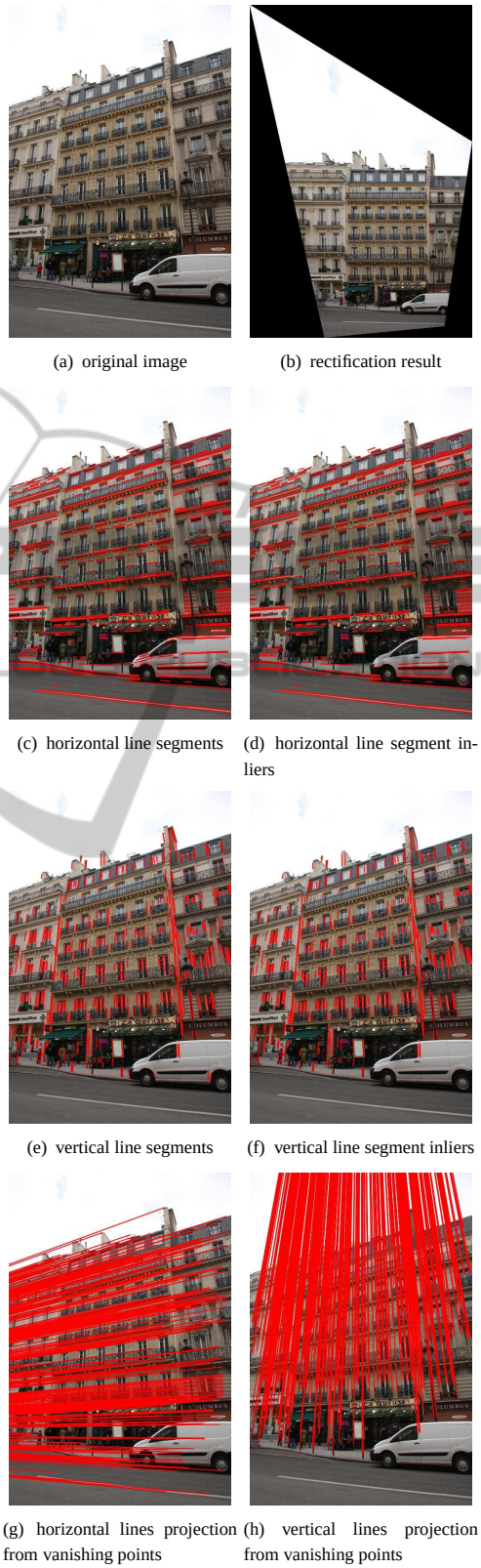

(a) original image (b) rectification result

(c) horizontal line segments (d) horizontal line segment inliers

(e) vertical line segments (f) vertical line segment inliers

(g) horizontal lines projection from vanishing points (h) vertical lines projection from vanishing points

Figure 3: Perspective rectification process.

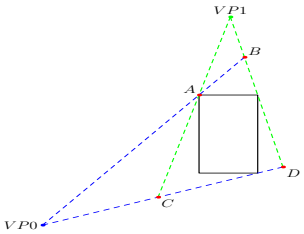

Figure 4: One configuration on two vanishing points.

minimize the effect from imperfect line segment samples. From figure 3(c), 3(d), 3(e) and 3(f), it can be seen that after RANSAC the number of line segments is reduced (especially on the roof and the ground floor near the car).

Algorithm 1: Line segment samples filtering using RANSAC.

Set number_inliers=0, angle_std=10e+5
Set angle_threshold=10°
Set N=1000, p=0.99
for $i = 0$ to N **do**
  Randomly select half of the line segments
  Calculate vanishing point using LM optimization
  Construct auxiliary line segment from vanishing point and middle point of the line segment
  Calculate the angle between the line segment and auxiliary line segment for all line segments
  if angle<angle_threshold **then**
    set it as inlier
  end if
  Calculate angle standard deviation for all inliers
  if (number_of_inliers $>$ number_inliers) || (number_of_inliers==number_inliers && inlier_angle_std $<$ angle_std) **then**
    update inliers
    update angle_std
  end if
  Set $e = 1 - number\_inliers/total\_lines$
  Set $N = 1log(1-p)/log(1-(1-e)^4)$
end for

3.3 Region of Interest Extraction

The next step is to extract the region of interest from the rectified image, which is the central region containing only the facade. (See figure 5) The procedure involves calculating new positions of four points of original image corners (upper left, upper right, lower left and lower right) in the rectified image. Connecting those four points in the rectified image will define a viewable quadrilateral region which is seen from the camera with no black pixel. From those four points, we can obtain a maximum rectangle inside the quadrilateral which is the region of interest.

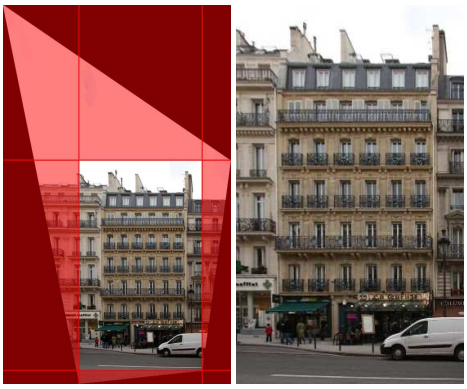

Figure 5: Region of interest extraction.

4 FACADE EXTRACTION

The facade extraction process consists of several steps. In this process, the sky above, the road underneath, and the neighbourhood building facades will be removed.

4.1 Sky Removal

4.1.1 Luminance Model

We assume the image can be divided into two parts based on the luminance distribution. One is bright as the sky and the other is dark as the facade beneath. Based on the large number law, the luminance distribution on the sky area and on the facade area will follow Gaussian distribution. It could be considered that every facade has its own unique facade wall decoration scheme, which defines consistent material use and color painting. Hence, the amount of light reflected from the facade wall should be around a mean value and perturbed with a certain deviation because the surface of the facade is not flat. Moreover, the sky could be considered as white regions with deviation from the soft cloud shades. Under extreme case, the sky is totally white which will have a mean value of maximum luminance and zero variance.

The problem of estimating the parameters of finite Gaussian mixture models has been extensively studied. We use the Expectation-Maximization method (Martinez, 2001) for estimating the means and variations, which is run iteratively. In each iteration, the mixing coefficients, the means and variances are computed. The iteration stops when it reaches the maxi-

mum iteration or the error metrics reach the specification.

4.1.2 Image Segmentation using MRF

After obtaining two groups of Gaussian parameters, the next step is to segment the image into sky and non-sky regions. This can be considered as a binary labeling problem. We define the labeling cost as using Gaussian distribution density functions with obtained Gaussian parameters. When we denote the sky luminance Gaussian distribution density function as $N(\mu_{sky}, \sigma_{sky})$, and the facade region luminance Gaussian distribution density function as $N(\mu_{facade}, \sigma_{facade})$, for a pixel with pixel value v, the cost of labeling it as sky is $N(v-\mu_{sky}, \sigma_{sky})$ and the cost of labeling it as facade is $N(v-\mu_{facade}, \sigma_{facade})$, the optimal labeling is achieved by minimizing the overall cost over all pixels by using Belief Propagation (Szeliski et al., 2008) by considering of the spatial consistency in four clique connections (up, down, left and right).

4.1.3 Skyline Extraction

After getting the binary segmented image, the sky line needs to be extracted. The first step is to apply morphology operation on the binary image to fill in some holes. Then the border curve between the sky and facade is extracted. The final position is fixed by averaging y coordinate of the border curve.

4.2 Road Removal

The road area is usually painted in dark gray, blue, or red. And it is less textured and decorated with white lanes. From figure 6, it can be seen that the line segments on the roads are more likely horizontal while on the building facades, line segments are both horizontal and vertical. Therefore, it is possible to use the direction of line segments to detect the road area.

4.2.1 Line Segment Model

We consider that below the road line position, there are less vertical line segments on the image. To define horizontal line segment density function along Y axis, the number of horizontal line segments below each vertical position is being counted and being divided by the total horizontal line segments quantity. The vertical line segment density function is also defined in this way. Then an object function for finding the road line can be defined as the ratio of two density functions in energy form as the shown below.

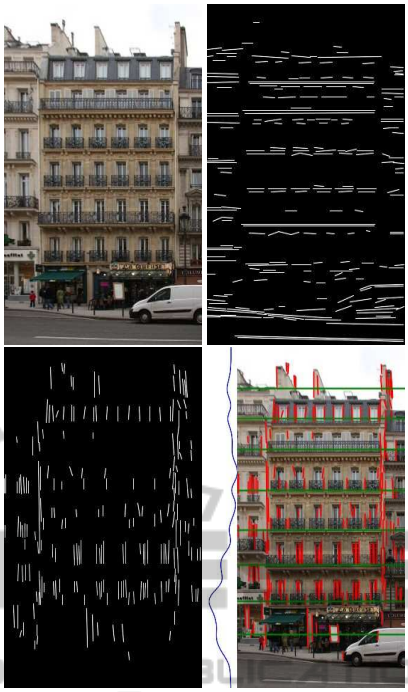

Figure 6: Horizontal and vertical line segments distribution for road line hypothesis.

$$E(y) = E_h(y)/E_v(y) \tag{2}$$

where $E_h(y)$ is defined as the ratio of the number of horizontal line segments $n_h(y)$ below y to the total number of horizontal line segments N_h, and $E_v(y)$ is defined the ratio of the number of vertical line segments $n_v(y)$ below y to the total number of vertical line segments N_v.

$$\begin{aligned} E_h(y) &= e^{n_h(y)/N_h} \\ E_v(y) &= e^{n_v(y)/N_v} \end{aligned} \tag{3}$$

4.2.2 Line Segment Profiling and Road Line Extraction

The energy function is evaluated vertically from the image top to the bottom to construct an energy profile. Then the obtained energy profile could be further smoothed to remove the small noises. From the profile (Figure 6, the most right image), the energy is shown to be high on horizontal ledges and on road line as expected.

The last local maximum on the energy profile should correspond to the road line because the road is always on the bottom of the image. The final position for the road line is fixed by averaging Y position from all the horizontal line segments below last local maximum.

4.3 Neighbourhood Removal

The last step is to extract the facades from the neighbourhood on its shoulder. On the image, the definition of facade vertical border can be quite ambiguous. Rain water pipe is a weak clue of the vertical separation under same cases. Here we take a strong assumption on the building layout that horizontal consistency breaks at building borders which works only in most Parisian urban areas.

4.3.1 Horizontal Line Segment Distribution Discontinuity as Symmetry Line and Facade Border Clues

Windows on facades are repeated horizontally. Consequently, the horizontal edges imposed by window top borders are also repeated. In the gaps between the windows horizontal edges, transitional symmetric lines and facade vertical borders are located. On the window transitional symmetric lines, the window arrangements on both the left and the right are similar. On the facade vertical borders, the windows arrangement on the left and on the right are different (asymmetric). (see Figure 7).

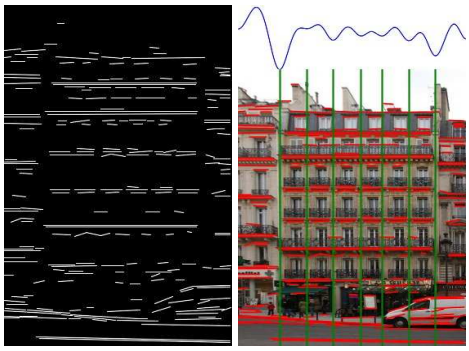

Figure 7: Horizontal line segments distribution.

We extract those gap positions as the hypothesis of facade separation lines. In order to locate the gaps, the horizontal line segment image is summed up along Y axis such that the X profile is obtained. After proper smoothing on this horizontal line segment profile, the local minima which correspond to the gaps between windows are extracted.

Afterwards, at each horizontal position, we measure the symmetry on its shoulders. We first sum up the horizontal line segments in a certain region on each horizontal position's shoulder along X axis, to the left and to the right separately to get two Y profiles. From two profiles on the left (a) and on the right (b), we can measure the symmetry. If the position is considered as an asymmetric line, it will be accepted as a facade border line. The symmetry measure is defined as follows.

$$Symmetry = \frac{\sum \delta(a_i b_i) * |a_i + b_i|}{\sum a_i + \sum b_i} \quad (4)$$

$\sum \delta(a_i b_i) * |a_i + b_i|$ sums the line segments symmetric to the separation line hypothesis. If the profiles are mostly different, there is less chance the line segments are aligned vertically from left and from right of the separation line, so less is contributed to the numerator of this symmetry measure. An empirical hard threshold of 0.5 is used that value no larger than 0.5 will be considered as asymmetric.

4.3.2 Border Line Determination and Facade Extraction

The borders between facades are extracted based on the following procedure. If two distinct asymmetric lines are found on the image border, they are treated as the facade borders. If one of them is missing or no asymmetric line is found, vertical line segment profile along the whole image is checked to pick up a position where a strong vertical line exists that is longer than one fourth of the image height. This vertical line is usually located where the rain water pipe is. If no strong lines are found, the image border is set to be the facade border.

5 RESULTS AND CONCLUSIONS

We have successfully applied our proposed method on all of the Haussmannian facades on the Soufflot Street in Paris.

We evaluate the rectification and extraction separately. The rectification is assessed by measuring mean angle of horizontal line segments and mean absolute difference between angle of vertical line segments and 90 degree in radians. And the extraction is evaluated by measuring the ratio of the intersection area against the union area from automatically extracted region and a ground truth region done manually. Results on four buildings (No. 11, 12, 19 and 26) are shown in the below table and Figure 8. The running time for rectification and segmentation is related to the number of line segments detected in images and also the image size. For a typical facade image in 518×778, it takes less than 2 minutes for rectification and extraction on a machine with 2.5GHz Dual-core processer and 2G RAM.

The main contributions of this paper are twofolds. One is we have proved that properly modeling of the

Table 1: Error metrics.

	b11	b12	b19	b26
$Angle_h$	0.045	0.046	0.037	0.044
$Angle_v$	0.035	0.037	0.041	0.048
Overlapping	85.43%	83.04%	92.78%	95.00%

Figure 8: Results on Soufflot Street Facades. Left to right, original, rectified, cropped, final and ground truth.

distribution of line segments will help the interpretation of the scene. The second contribution is that we presented fast efficient methods of rectification and segmentation process which require less human interactions, and proved to be useful for many urban modeling and urbanism applications as well.

One of the limitations of our current method, however, is that it is scale sensitive. Another limitation is in the road detection which still depends on the assumption that the road should be rather clean with less occlusion from cars.

REFERENCES

Grompone von Gioi, R., Jakubowicz, J., Morel, J. M., and Randall, G. (2010). LSD: A Fast Line Segment Detector with a False Detection Control. *IEEE Transactions on Pattern Analysis and Machine Intelligence*, 32(4):722–732.

Hoiem, D., Efros, A. A., and Hebert, M. (2005). Geometric context from a single image. In *International Conference of Computer Vision (ICCV)*, volume 1, pages 654 – 661. IEEE.

Kalantaria, M., Jung, F., Paparoditis, N., and Guedon, J. (2008). Robust and automatic vanishing points detection with their uncertainties from a single uncalibrated image, by planes extraction on the unit sphere. In *ISPRS08*, page B3a: 203 ff.

Laungrungthip, N. (2008). Sky detection in images for solar exposure prediction.

Laungrungthip, N., McKinnon, A., Churcher, C., and Unsworth, K. (2008). Edge-based detection of sky regions in images for solar exposure prediction. In *IVCNZ08*, pages 1–6.

Liebowitz, D. and Zisserman, A. (1998). Metric rectification for perspective images of planes. In *Proceedings of the IEEE Computer Society Conference on Computer Vision and Pattern Recognition*, CVPR '98, pages 482–, Washington, DC, USA. IEEE Computer Society.

Martinez, W. (2001). *Computational Statistics Handbook with Matlab*. CRC Press, Boca Raton.

Matas, J., Galambos, C., and Kittler, J. (1998). Progressive probabilistic hough transform.

Quartulli, M. and Datcu, M. (2004). Stochastic Geometrical Modeling for Built-Up Area Understanding From a Single SAR Intensity Image With Meter Resolution. *IEEE Transactions on Geoscience and Remote Sensing*, 42:1996–2003.

Schmitt, F. and Priese, L. (2009). Sky detection in csc-segmented color images. In *VISAPP (2)*, pages 101–106.

Szeliski, R., Zabih, R., Scharstein, D., Veksler, O., Kolmogorov, V., Agarwala, A., Tappen, M., and Rother, C. (2008). A comparative study of energy minimization methods for markov random fields with smoothness-based priors. *IEEE Trans. Pattern Anal. Mach. Intell.*, 30:1068–1080.

Zafarifar, B. and de With, P. (2006). Blue Sky Detection for Picture Quality Enhancement. pages 522–532.